NRC Research Press

ARTICLE

A solid-state ^{17}O NMR study of platinum-carboxylate complexes: carboplatin and oxaliplatin

Xianqi Kong, Victor Terskikh, Abouzar Toubaei, and Gang Wu

Abstract: We report synthesis and solid-state NMR characterization of two ^{17}O-labeled platinum anticancer drugs: cis-diammine(1,1-cyclobutane-[$^{17}O_4$]dicarboxylato)platinum(II) (carboplatin) and ([$^{17}O_4$]oxalato)[(1*R*, 2*R*)-(–)-1,2-cyclohexanediamine)]platinum(II) (oxaliplatin). Both ^{17}O chemical shift (CS) and quadrupolar coupling (QC) tensors were measured for the carboxylate groups in these two compounds. With the aid of plane wave DFT computations, the ^{17}O CS and QC tensor orientations were determined in the molecular frame of reference. Significant changes in the ^{17}O CS and QC tensors were observed for the carboxylate oxygen atom upon its coordination to Pt(II). In particular, the ^{17}O isotropic chemical shifts for the oxygen atoms directly bonded to Pt(II) are found to be smaller (more shielded) by 200 ppm than those for the non-Pt-coordinated oxygen atoms within the same carboxylate group. Examination of the ^{17}O CS tensor components reveals that such a large ^{17}O coordination shift is primarily due to the shielding increase along the direction that is within the O=C–O–Pt plane and perpendicular to the O–Pt bond. This result is interpreted as due to the σ donation from the oxygen nonbonding orbital (electron lone pair) to the Pt(II) empty d_{yz} orbital, which results in large energy gaps between σ(Pt–O) and unoccupied molecular orbitals, thus reducing the paramagnetic shielding contribution along the direction perpendicular to the O–Pt bond. We found that the ^{17}O QC tensor of the carboxylate oxygen is also sensitive to Pt(II) coordination, and that ^{17}O CS and QC tensors provide complementary information about the O–Pt bonding.

Key words: solid-state NMR, oxygen-17, tensor, anticancer drug, platinum-carboxylate complex.

Résumé : Nous présentons la synthèse et la caractérisation par RMN du solide de deux médicaments anticancéreux radiomarqués à l'oxygène-17 (^{17}O) à base de platine : le cis-diammine(1,1-cyclobutane-[$^{17}O_4$]dicarboxylato)platine(II) [carboplatine] et le ([$^{17}O_4$]oxalato)[(1R,2R)-(–)-1,2-cyclohexanediamine)]platine(II) [oxaliplatine]. Nous avons mesuré les tenseurs de déplacement chimique et de couplage quadrupolaire de l'^{17}O relatifs aux groupements carboxylate de ces deux composés. À l'aide de calculs fondés sur la théorie de la fonctionnelle de la densité à base d'ondes planes, nous avons déterminé les orientations des tenseurs de déplacement chimique et de couplage quadrupolaire de l'^{17}O dans le cadre de référence moléculaire. Nous avons observé des variations importantes de ces tenseurs relatifs aux atomes d'oxygène des groupements carboxylate au moment de leur coordination à l'atome Pt(II). En particulier, on observe que les déplacements chimiques isotropiques de l'^{17}O relatifs aux atomes d'oxygène directement liés à l'atome de Pt(II) sont plus faibles (blindés) de 200 ppm que ceux relatifs aux atomes d'oxygène faisant partie du même groupement carboxylate mais qui ne sont pas coordonnés à l'atome de platine. L'examen des composantes du tenseur de déplacement chimique de l'^{17}O révèle que la grande amplitude du déplacement chimique de l'^{17}O au moment de la coordination est principalement le fait d'une augmentation du blindage dans la direction parallèle au plan O=C-O–Pt et perpendiculaire à la liaison O-Pt. Ces résultats sont interprétés comme étant attribuables à l'effet inductif donneur s de l'orbitale non liante de l'atome d'oxygène (doublet non liant) à l'orbitale vide d_{yz} de l'atome de Pt(II), donnant lieu à un large bande interdite entre l'orbitale s(Pt–O) et les orbitales moléculaires vacantes, et de fait, réduisant la contribution du blindage paramagnétique dans la direction perpendiculaire à la liaison O–Pt. Nous avons observé que le tenseur de coupage quadripolaire de l'^{17}O des atomes d'oxygène des groupements carboxylate est aussi sensible à la coordination au Pt(II) et que les tenseurs de déplacement chimique et de couplage quadrupolaire de l'^{17}O fournissent des renseignements complémentaires à propos de la liaison O–Pt. [Traduit par la Rédaction]

Mots-clés : RMN du solide, oxygène-17, tenseur, médicament anticancéreux, complexe de carboxylate de platine.

Introduction

In recent years, solid-state ^{17}O NMR spectroscopy has been shown to be a useful technique for direct detection and characterization of oxygen nuclei in organic and biological molecules.[1–4] The remarkable sensitivity of ^{17}O quadrupolar coupling (QC) and chemical shift (CS) tensors toward molecular interactions such as hydrogen bonding and metal-ligand interactions makes ^{17}O an important NMR probe, capable of providing information that sometimes is difficult to obtain with the more conventional ^{1}H, ^{13}C, and ^{15}N NMR studies. Over the past decade, ^{17}O QC and CS tensors have been experimentally determined for many oxygen-containing organic functional groups. At the present time the solid-state ^{17}O NMR method finds its use not only for studying protein-ligand complexes,[5] but also for obtaining dynamic information about molecular motions in organic solids.[6] The most recent advances in solid-state ^{17}O NMR include studies of pharmaceuticals[7,8] and paramagnetic coordination compounds.[9] Another significant recent development is the application of dynamic nuclear polarization

Received 9 January 2015. Accepted 27 February 2015.

X. Kong, A. Toubaei, and G. Wu. Department of Chemistry, Queen's University, 90 Bader Lane, Kingston, ON K7L 3N6, Canada.
V. Terskikh. Department of Chemistry, Queen's University, 90 Bader Lane, Kingston, ON K7L 3N6, Canada; Department of Chemistry, University of Ottawa, Ottawa, ON K1N 6N5, Canada.
Corresponding author: Gang Wu (e-mail: gang.wu@chem.queensu.ca).

This article is part of a Special Issue in honour of Dr. John Ripmeester and his outstanding contributions to science.

Scheme 1. Molecular structures of carboplatin and oxaliplatin.

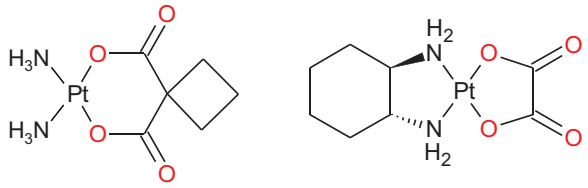

(DNP) to drastically boost the sensitivity of solid-state ^{17}O NMR experiments.[10–12]

In the present work, we use solid-state ^{17}O NMR to study two platinum anticancer drugs: carboplatin and oxaliplatin (Scheme 1). Although several thousand platinum-based anticancer drug molecules have been developed in research laboratories over the past 30 years, only about two dozen have ever gone into clinical trials. Carboplatin and oxaliplatin are the only two Pt compounds that have gained international marketing approval.[13] Both carboplatin and oxaliplatin show significantly less toxicity than cisplatin, the first commercial platinum-based drug. While both solution and solid-state NMR techniques utilizing ^{1}H, ^{13}C, $^{14/15}$N, ^{195}Pt, and ^{35}Cl as nuclear probes have been extensively employed to study Pt anticancer drugs,[14–19] ^{17}O NMR has not yet been explored in the studies of this class of drug molecules.

In carboplatin and oxaliplatin, the mode of bonding between the carboxylate group and the Pt(II) metal center can be described as being monodentate, O=C–O–Pt(II), where the 4 atoms are essentially in the same plane. While there have been a number of experimental solid-state ^{17}O NMR and computational studies on the ^{17}O QC and CS tensors in carboxylic acids and their salts,[20–35] none of the previous studies have dealt with a carboxylate (–COO$^-$) group bound to Pt(II). The primary goals of the present study are (*i*) to experimentally determine the ^{17}O CS and QC tensors in these important Pt(II) anticancer drugs and (*ii*) to examine the effect of bonding to a transition metal on these ^{17}O NMR tensors. In carboplatin and oxaliplatin, since the mode of bonding is O=C–O–Pt(II), the non-Pt-coordinated oxygen atom can serve as an internal reference, making it easier to examine the effect of metal binding on ^{17}O NMR tensors. Another reason for us to choose these two platinum anticancer drugs is that their crystal structures have been reported.[36,37] The known crystal structures would allow us to perform plane wave DFT calculations of the ^{17}O NMR tensors in these compounds. These calculations have been proven to produce reliable tensor orientations in the molecular frame of reference and thus can aid the interpretation of the experimental data.

Experimental section

Synthesis of ^{17}O-labeled Pt(II) complexes

Preparations of [$^{17}O_4$]carboplatin and [$^{17}O_4$]oxaliplain were carried out by following literature procedures[38,39] with necessary modifications for ^{17}O isotopic incorporation. Schematic diagrams illustrating the employed synthetic strategies are given in the Supplementary data, and the synthetic details are described below.

Dipotassium 1,1-cyclobutane-[$^{17}O_4$]-dicarboxylate

1,1-Cyclobutanedicarboxylic acid (300 mg) was dissolved in 40% ^{17}O-enriched water (310 μL, purchased from CortecNet) and heated at 80 °C for 22 h. After cooling to room temperature (RT), the solution was neutralized by addition of a solution of KOH (233 mg) in EtOH (8 mL). After the mixture was left in a refrigerator for 20 min, the white solid was collected by filtration, washed with EtOH (3 × 3 mL), and then dried under vacuum. A total of 366 mg of the title compound were obtained.

[$^{17}O_4$]Carboplatin

cis-Diaminodiiodoplatinum(II) (567 mg, 1.17 mmol) and $AgNO_3$ (400 mg, 2.34 mmol) were added to H_2O (30 mL), and the solution was stirred in an oil bath at 45–50 °C (under darkness) for 3 h. After cooling to RT, the insoluble material was removed by filtration through a pad of Celite. The filter pad was washed with H_2O (5 mL). The filtrate and washing were combined in a flask containing dipotassium 1,1-cyclobutane-[$^{17}O_4$]-dicarboxylate (244 mg, 1.10 mmol), forming a clear solution. The mixture was concentrated to dryness on a rotary evaporator at 55 °C. The residual material was treated in H_2O (5 mL) followed by addition of 2 drops of 30% ammonium hydroxide solution. The mixture was heated briefly to dissolve most of the solid and filtered (a small amount of yellowish insoluble material was thus removed), and the filtrate was concentrated to dryness. The residual material was treated with H_2O (1 mL), heated briefly, then cooled to 4 °C. The solid material was collected, washed with cold H_2O (2 × 0.5 mL) and ethanol (0.5 mL), and dried under vacuum. The title compound was obtained as a white, free-flow crystalline solid (220 mg, yield 54%). ^{1}H NMR (500 MHz, D_2O): δ 1.80 ppm (qt, 2H, J = 7.75 Hz), 2.78 ppm (t, 4H, J = 7.75 Hz). ^{17}O NMR (67.7 MHz, D_2O): δ 126.8 ppm (br, 2O), 310.0 ppm (br, 2O). The ^{17}O NMR spectrum is shown in the Supplementary data.

Dipotassium [$^{17}O_4$]oxalate

Oxalic acid (1.2 g) was treated with a mixture of 40% ^{17}O-enriched water (1 mL) and 1,4-dioxane (10 mL) at 60 °C for 66 h. After the solvent was recovered with an N_2 flow passing through the flask into a cold trap, 2.3 g of solid was obtained (46% of the mass was residual solvent). This solid material was then added to a solution of KOH (2.0 g) in water (10 mL). The solution was concentrated (rotary evaporation at <50 °C) to a solid residue, which was further treated with EtOH (25 mL). The white solid was collected by filtration and washed with EtOH (3 × 10 mL). After drying the solid, a total of 2.3 g of the title compound were obtained.

[$^{17}O_4$]Oxaliplatin

Dichloro(*R,R*-cyclohexane-1,2-diamine)platinum(II) (540 mg, 1.42 mmol) and $AgNO_3$ (460 mg, 2.70 mmol) were added to 30 mL of H_2O. In the dark, the mixture was stirred in an oil bath at 90 °C for 5 min, and then cooled for over 1 h to RT. The mixture was stirred at RT overnight. Insoluble material was removed by filtration through a pad of Celite, and then the pad was washed with H_2O (5 mL). The filtrate was collected in a 100 mL flask, to which dipotassium [$^{17}O_4$]oxalate (220 mg, 1.32 mmol) was then added. The mixture was concentrated to dryness on a rotary evaporator at 35–40 °C. The residual material was treated with H_2O (5 mL). The solid material was collected by filtration and washed with cold H_2O (4 × 3 mL, and 2 × 4 mL). After drying the solid under vacuum, the title compound was obtained as a white powder (285 mg, yield 54%). ^{1}H NMR (600 MHz, D_2O): δ 1.01 (m, 2H), 1.15 (m, 2H), 1.42 (m, 2H), 1.90 (m, 2H), 2.20 (m, 2H). Note that the NH_2 protons were not observed. ^{17}O NMR (81.0 MHz, D_2O): δ 134.7 (br, 2O), 306.9 (br, 2O). The ^{17}O NMR spectrum is shown in the Supplementary data.

Solid-state ^{17}O NMR

Solid-state ^{17}O NMR experiments were performed on Bruker Avance-600 (14.1 T) and Bruker Avance-II 900 (21.1 T) NMR spectrometers. A Hahn-echo sequence was used for both static and magic-angle spinning (MAS) experiments to eliminate the acoustic ringing from the probe. Effective 90° pulses of 1.7 and 1.0 μs were used for the ^{17}O central transition (CT) experiments at 14.1 and 21.1 T, respectively. The ^{17}O MAS NMR spectra at 14.1 T were performed using a 4 mm Bruker MAS probe at a spinning frequency of 14.5 kHz. The ^{17}O MAS NMR spectra at 21.1 T were obtained with a 1.3 mm Bruker MAS probe at a sample spinning frequency of 50.0 kHz. Static experiments at 14.1 T were performed with the 4 mm MAS probe, and powder samples were packed in 4 mm rotors. At 21.1 T, a homebuilt 5 mm H/X

Fig. 1. (Colour online) Experimental (blue trace) and simulated (red trace) ^{17}O MAS NMR spectra of (*a*) [$^{17}O_4$]carboplatin and (*b*) [$^{17}O_4$]oxaliplatin at two magnetic fields. The simulated spectra for individual sites are shown in green and purple. The sample spinning frequencies were 14.5 and 50.0 kHz for experiments at 14.1 and 21.1 T, respectively. For each compound, the same ^{17}O NMR parameters as summarized in Table 1 were used to simulate the spectra recorded at two magnetic fields. Note that the spinning sidebands are clearly visible in the simulated spectra at 14.1 T. Other data acquisition parameters are given in the text.

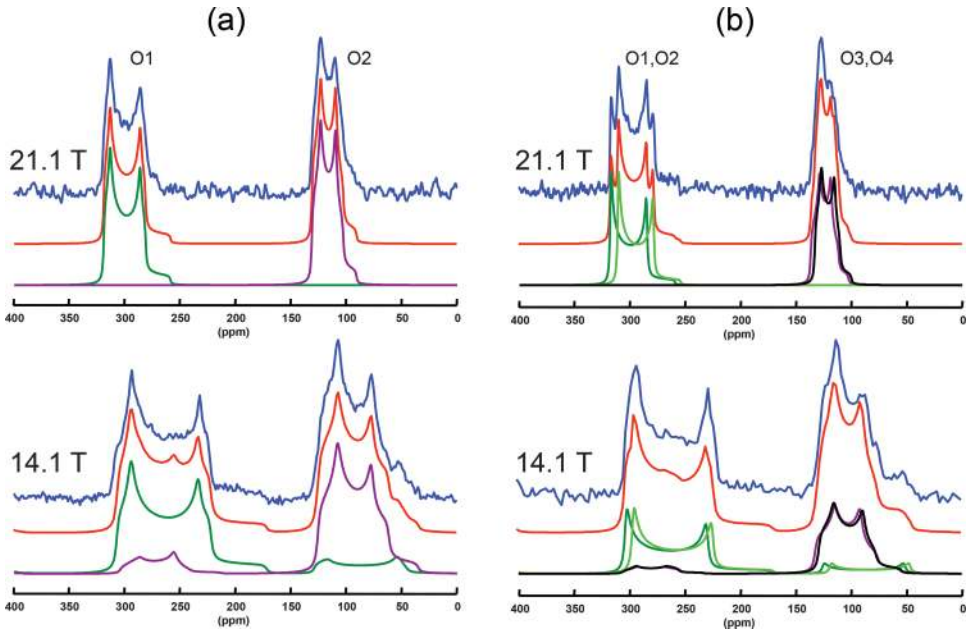

Table 1. Experimental and computed ^{17}O CS[a] and QC[b] NMR tensor parameters[c] for carboplatin and oxaliplatin.

Compound	δ (ppm)[d]	δ_{iso} (ppm)	δ_{11} (ppm)	δ_{22} (ppm)	δ_{33} (ppm)	C_Q (MHz)	η_Q
Carboplatin							
C=O1							
Exptl.	310.0	326(1)	522(5)	422(5)	34(5)	8.15(2)	0.15(5)
CASTEP		327	523	433	25	8.145	0.318
C–O2–Pt							
Exptl.	126.8	134(1)	369(5)	99(5)	−66(5)	−6.50(2)	0.33(5)
CASTEP		184	431	149	−26	−6.442	0.286
Oxaliplatin							
C=O1							
Exptl.	306.9	327(1)	503(5)[e]	425(5)[e]	41(5)[e]	8.20(2)	≤0.05
CASTEP		336	508	450	48	8.383	0.147
C=O2							
Exptl.	306.9	320(1)	—	—	—	8.10(2)	0.00(5)
CASTEP		328	495	436	51	8.231	0.189
C–O3–Pt							
Exptl.	134.7	138(1)	411(5)[f]	64(5)[f]	−67(5)[f]	−5.90(2)	0.40(5)
CASTEP		190	457	140	−26	−6.150	0.296
C–O4–Pt							
Exptl.	134.7	135(1)	—	—	—	−5.90(2)	0.30(5)
CASTEP		184	449	127	−24	−6.131	0.372

Note: The estimated errors for experimental data are shown in parentheses.

[a]Computed chemical shifts (δ) were obtained from computed shielding values (σ) by using $\delta = \sigma_{ref} - \sigma$, where σ_{ref} was chosen to be 290.0 ppm so that the trend line relating the computed and experimental chemical shift data passes the origin.

[b]The sign of C_Q was assumed to be the same as the computed one.

[c]For both compounds, the experimental Euler angles that define the relative orientation between the ^{17}O QC and CS tensors are: C=O, $\alpha = 0$, $\beta = 90 \pm 5$, $\gamma = 60 \pm 10°$; C–O–Pt, $\alpha = 0$, $\beta = 90 \pm 5$, $\gamma = 40 \pm 10°$.

[d]Measured in D_2O at 298 K.

[e]Averaged values between O1 and O2.

[f]Averaged values between O3 and O4.

solenoid probe was used for static experiments, and solid samples were packed into a 5 mm Teflon tube to reduce the background signal. High-power CW ^1H decoupling (70 kHz) was applied in all static experiments. For carboplatin at 21.1 T, the recycle delay was 20 s, and a total of 512 transients were accumulated for both static and MAS spectra. For oxaliplatin at 21.1 T, the recycle delay was 60 s for both static and MAS spectra. A total of 896 transients and 1500 transients were accumulated in the static and MAS experiments, respectively. For carboplatin at 14.1 T, the recycle delay was 5 s for collecting both static (8348 transients) and MAS

(10 355 transients) spectra. For oxaliplatin at 14.1 T, the recycle delay was 30 s in the static (1784 transients) and MAS (1080 transients) experiments. A liquid H_2O sample was used for both RF power calibration and ^{17}O chemical shift referencing (δ = 0 ppm). All spectral simulations were performed with DMfit.[40]

Computational details

Plane wave pseudopotential DFT calculations of the NMR shielding and electric field gradient parameters were performed using the Cambridge Serial Total Energy Package (CASTEP) software and Materials Studio 4.4 program (Accelrys)[41,42] on a HP xw4400 workstation with a single Intel Dual-Core 2.67 GHz processor and 8 GB DDR RAM. The Perdew, Burke, and Ernzerhof (PBE) functionals was used in all calculations in the generalized gradient approximation (GGA) for the exchange correlation energy.[43,44] On-the-fly pseudopotentials were used as supplied with NMR CASTEP with a plane wave basis set cut-off energy of 550 eV, and the Monkhorst-Pack *k*-space grid sizes of 3 × 2 × 2 (2 *k*-points used) and 2 × 3 × 3 (9 *k*-points used) for carboplatin and oxaliplatin, respectively. The reported crystal structures of carboplatin[36] and oxaliplatin[37] were used as starting structures, and then geometry optimization was performed using the BFGS method[45] without the cell optimization. The following convergence tolerance parameters were used in the geometry optimization process: total energy 5 × 10^{-5} eV/atom, maximum displacement 0.005 Å, maximum force 0.1 eV/Å, and maximum stress 0.2 GPa. Nuclear magnetic shielding calculations were also performed with the Amsterdam Density Functional (ADF, version 2012)[46] software package. Vosko–Wilk–Nusair (VWN) exchange-correlation functional[47] was used for the local density approximation (LDA), and the PBE exchange-correlation functionals[43,44] was applied for the generalized gradient approximation (GGA). Standard Slater-type orbital (STO) basis sets with triple-zeta quality plus polarization functions (TZ2P) were used for all the atoms. The spin orbital relativistic effect was incorporated via the zero-order regular approximation (ZORA).[48–51] The ADF calculations were carried out on Sun SPARC Enterprise M9000 servers at the High Performance Computing Virtual Laboratory (HPCVL) of Queen's University. Each of the servers consists of 64 quad-core 2.52 GHz sparc64 VII processors with 8 GB of RAM per core (2 TB of total memory).

Results and discussion

Experimental determination of ^{17}O NMR tensors

The general solid-state NMR approach for the experimental characterization of ^{17}O CS and QC tensors consists of two steps. First, one obtains good-quality ^{17}O NMR spectra under the MAS condition, from which the values of δ_{iso}, C_Q, and η_Q can be obtained for each oxygen site. Second, one records ^{17}O static NMR spectra preferably at multiple magnetic fields. An analysis of the static spectra would allow determination of the ^{17}O CS tensor components (δ_{11}, δ_{22}, δ_{33}) and their relative orientations with respect to the QC tensor. A detailed theoretical background can be found in the literature.[52,53] Figure 1 shows the ^{17}O MAS spectra obtained for [$^{17}O_4$]carboplatin and [$^{17}O_4$]oxaliplatin at two magnetic fields. In each MAS spectrum, two groups of signals were observed, corresponding to the two types of oxygen atoms (directly Pt-bonded and non-Pt-coordinated) in carboplatin and oxaliplatin. At 14.1 T, since the sample spinning frequency was only 14.5 kHz, weak spinning sidebands are visible for each central band from the simulated spectra. As these weak spinning sidebands happen to overlap with the central bands, they somewhat obscure the fine spectral features. At 21.1 T, in contrast, the sample spinning frequency was 50 kHz, and the MAS spectra, now free of spinning sidebands, exhibit very high spectral resolutions. It is interesting to note that while two oxygen sites are observed for carboplatin, a total of 4 oxygen sites (2 pairs) are detected for oxaliplatin. The crystal structure of carboplatin[36] indicates the presence of a mirror plane that contains the Pt(II) center and the

Fig. 2. (Colour online) Experimental (blue trace) and simulated (red trace) ^{17}O static NMR spectra of (*a*) [$^{17}O_4$]carboplatin and (*b*) [$^{17}O_4$]oxaliplatin at 21.1 T. The simulated spectra for individual sites are shown as dotted traces in green and purple. The data acquisition parameters are given in the text. The simulation parameters are summarized in Table 1. The corresponding static spectra recorded at 14.1 T together with spectral simulations are provided in the Supplementary data.

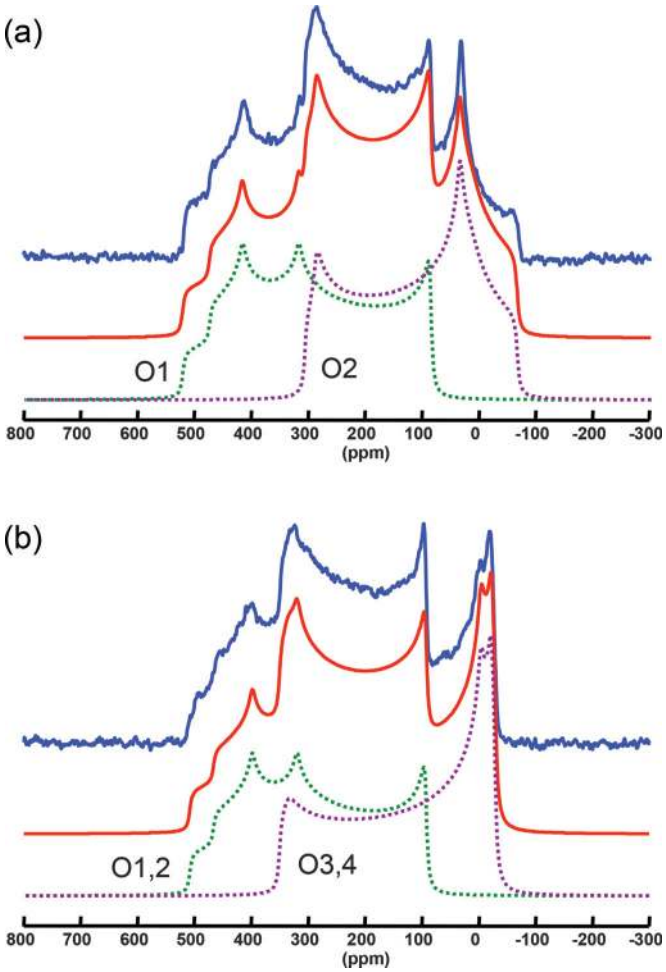

average cyclobutane ring bisecting the molecule. As a result, the two carboxylate groups in carboplatin are symmetry related. In comparison, the crystal structure of oxaliplatin[37] suggests that all 4 oxygen atoms of the oxalate group are crystallographically distinct. Therefore, the solid-state ^{17}O NMR observations shown in Fig. 1 are in agreement with the crystal structures of these compounds. As also seen from Fig. 1, experimental MAS spectra recorded at two magnetic fields for the same compound are matched very well by the simulated ones using the same set of NMR parameters. The experimental values of δ_{iso}, C_Q, and η_Q are summarized in Table 1. In general, carboplatin and oxaliplatin exhibit similar ^{17}O NMR parameters. The most interesting finding is that the ^{17}O chemical shifts for the oxygen atoms directly bonded to Pt(II) and the non-Pt-coordinated oxygen atoms differ by 200 ppm (vide infra); also see the solution ^{17}O spectra of these compounds in the Supplementary data. The directly Pt-bonded oxygens exhibit smaller C_Q values (ca. $|C_Q| \approx$ 6 MHz) than do the non-coordinated oxygens ($|C_Q| \approx$ 8 MHz), in agreement with previous observations on the effect from metal-ligand interactions.[54] It is important to note that the sign of C_Q cannot be readily determined simply from MAS and static spectra.

Figure 2 shows the ^{17}O static NMR spectra of carboplatin and oxaliplatin recorded at 21.1 T. Similarly, the static spectra were

Fig. 3. Depiction of the ^{17}O QC (*a*) and CS (*b*) tensor orientations in the molecular frames of reference of carboplatin. The QC tensor components are defined as $|\chi_{zz}| \geq |\chi_{yy}| \geq |\chi_{xx}|$. For comparison, the ^{17}O QC and CS tensor orientations in the O=C–O–H moiety of α-oxalic acid dihydrate[23] are shown in (*c*) and (*d*), respectively. The actual tensor eigenvalues are shown in parentheses. In (*b*) and (*d*), δ_{33} components are not shown for clarity.

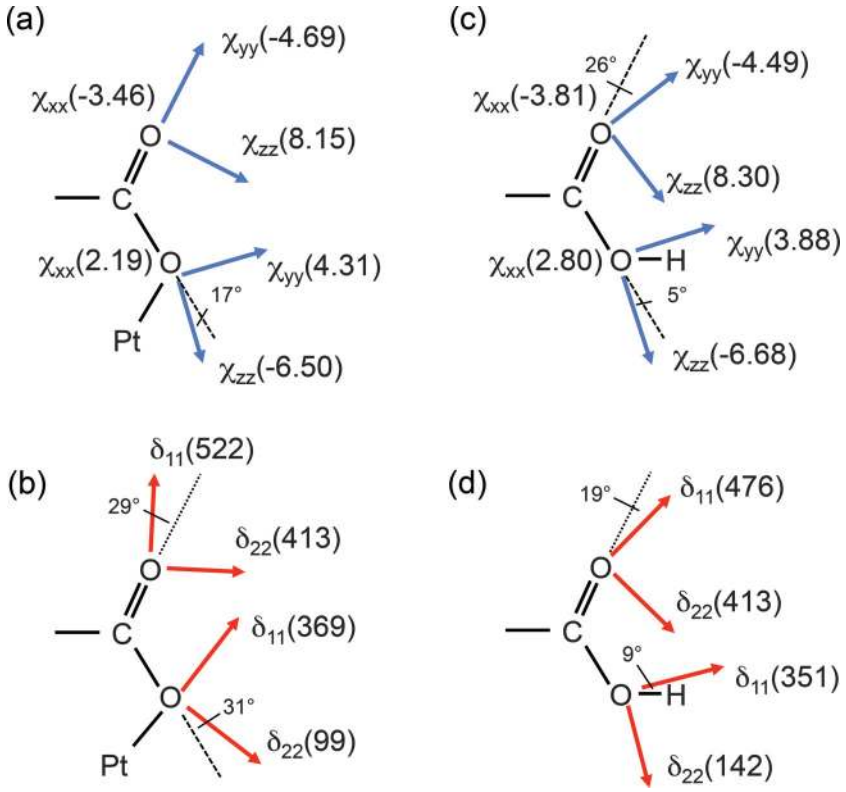

also obtained at 14.1 T (shown in the Supplementary data). Because of the low resolution in the static spectra, it was not possible to treat all 4 crystallographically distinct oxygen sites in oxaliplatin individually. Thus we assumed only 2 CS tensors (O1/O2 and O3/O4) in the spectral simulation. As seen from Fig. 2, the general agreement between experimental and simulated static spectra is satisfactory. Again, all experimental ^{17}O CS tensor components for carboplatin and oxaliplatin are listed in Table 1.

Plane wave DFT calculations and the tensor orientations

As the crystal structures for carboplatin and oxaliplatin are known, we performed plane wave DFT calculations using the CASTEP program.[41,42] This approach will produce results that can be directly compared with solid-state NMR data without any assumption on the size of the molecular cluster. The CASTEP results for ^{17}O NMR tensors are summarized in Table 1. In general, the computational results are in good agreement with the experimental data. A correlation plot (slope = 0.964; R^2 = 0.988) between experimental and computed ^{17}O CS tensor components is given in the Supplementary data. We should point out that the agreement between calculated and experimental results is clearly better for the non-Pt-coordinated oxygen atoms than for the directly Pt-coordinated ones, which is likely due to the neglect of relativistic effects in the CASTEP calculations. The computations also reveal a sign change in C_Q between the 2 types of oxygen atoms. For the non-Pt-coordinated oxygen atom, C_Q is positive, and it becomes negative for the directly Pt-bonded oxygen (*vide infra*).

Another benefit of the CASTEP calculations is that the ^{17}O CS and QC tensor orientations can be unambiguously determined in the molecular frame of reference. As we have shown previously,[52,54–57] the absolute orientations of the ^{17}O NMR tensors in the molecular frame of reference can be reliably predicted by modern quantum chemical calculations. The CASTEP results for the tensor orientations in carboplatin and oxaliplatin are depicted in Fig. 3.

Fig. 4. Comparison of ^{17}O ligand isotropic coordination shifts among monodentate carboxylate-metal complexes. The chemical shift difference between the two types of oxygen atoms in carboxylic acids (O=C–O–H) is also shown for completeness.

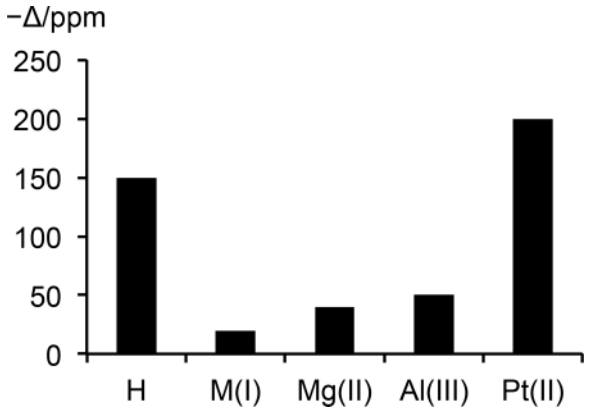

For the non-Pt-coordinated oxygen atom, χ_{zz} and χ_{yy} both lie in the O=C–O plane, being perpendicular to and along the C=O bond, respectively. This makes χ_{xx} perpendicular to the O=C–O plane. This ^{17}O QC tensor orientation is typical of a carbonyl functional group. The ^{17}O QC tensor orientation is quite different for the chelating oxygen, for which the χ_{zz} component is in plane but essentially along the C–O bond. The ^{17}O CS tensors are also quite different for the two types of oxygen atoms. For the directly Pt-bonded oxygen atom, δ_{11} of the ^{17}O CS tensor is oriented along the

Fig. 5. (*a*) Definition of the tensor components (∥, ⊥, π) in a carboxylate group; see text. Comparison of the ^{17}O QC (*b*) and CS (*c*) tensor components between the non-Pt-coordinated and directly Pt-bonded oxygen atoms in Carboplatin.

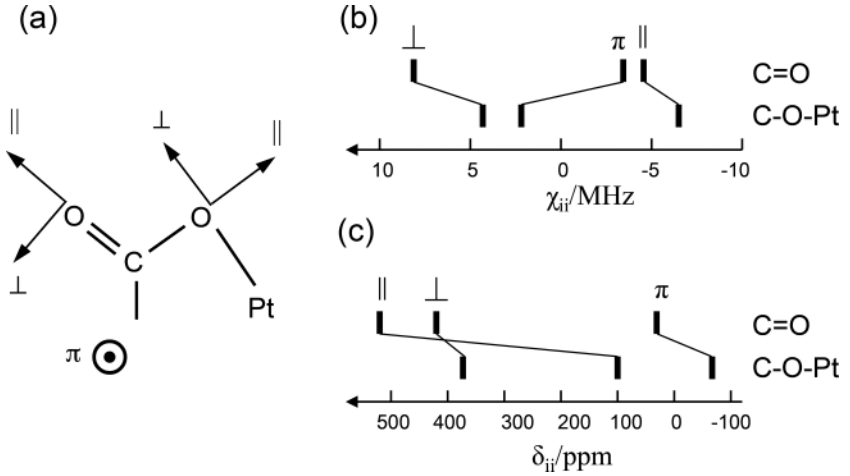

O–Pt bond, which makes it nearly perpendicular to the C–O bond. In comparison, δ_{11} is about 29° off the C=O bond for the non-Pt-coordinated oxygen. For both types of oxygen atoms, δ_{33} is always perpendicular to the O=C–O plane. These tensor orientations are in general agreement with the previous results on carboxylates.[2] It is especially worth noting that the ^{17}O NMR tensor orientations found in carboplatin and oxaliplatin are very similar to those in α-oxalic acid dihydrate determined from a single-crystal ^{17}O NMR study[23] (see Fig. 3). This similarity suggests that the O-Pt coordination bond in O=C–O–Pt resembles the O–H covalent bond in O=C–O–H (vide infra).

It is also worth commenting on the sign change in C_Q noted earlier. Since the definition of C_Q is associated with the largest QC component (in its absolute value), the apparent sign change from 8.15 MHz for the non-Pt-coordinated oxygen to –6.50 MHz for the directly Pt-bonded oxygen does not mean that the net change in C_Q is 8.15–(–6.50) = 14.65 MHz. Rather, one must examine the individual ^{17}O QC tensor components using the respective C–O bond as the frame of reference. As seen from Fig. 3, the changes in the 3 directions with respect to the C–O bond are: along the C–O bond, –6.50–(–4.69) = –1.81 MHz; perpendicular to the C–O bond but in the O–C–O plane, 4.31–8.15 = –3.84 MHz; perpendicular to the O–C–O plane, 2.19–(–3.46) = 5.65 MHz. Thus, the largest change is 5.65 MHz, occurring in the direction perpendicular to the O–C–O plane.

A survey of ^{17}O coordination shifts from carboxylate-metal interactions

As mentioned in the previous section, the most interesting result in this study is the 200 ppm difference in $\delta_{iso}(^{17}O)$ between the directly Pt-bonded and non-Pt-coordinated oxygen atoms. To put this in perspective, we surveyed the solid-state ^{17}O NMR data in the literature for metal-carboxylate interactions. To make direct comparison of NMR data from different compounds meaningful, we focused only on those carboxylates that exhibit the monodentate mode of binding to the metal ion, i.e., O=C–O–M^{+n}. To aid discussion, we define an ^{17}O coordination shift (Δ) as $\Delta = \delta_{iso}$(C–O–M^{+n}) – δ_{iso}(O=C). As illustrated in Fig. 4, for alkali metals, M^+, Δ is typically –20 ppm. For example, Wong et al.[31] reported the ^{17}O chemical shifts for the bound and noncoordinated oxygens in lithium β-oxalate are –249.6 and –265.0 ppm, respectively. For Mg(II)- and Al(III)-carboxylate interactions, Zhu and Wu observed that the ^{17}O coordination shifts are on the order of –50 and –60 ppm, respectively.[58] To make the comparison complete, Fig. 4 also shows that the chemical shift difference found in free carboxylic acid (O=C–O–H) where the "chelating" oxygen atom actually forms a covalent bond with H. In this case, the corresponding ^{17}O chemical shift difference is typically –150 ppm. In this context, the observed ^{17}O coordination shift of –200 ppm in carboplatin and oxaliplatin is quite remarkable and deserves further investigation as presented in the next section. We should also note that large negative ^{17}O coordination shifts have been previously reported in several solution ^{17}O NMR studies for oxygen-containing ligands bound to transition metals.[59–63] For example, Laurenczy et al.[52] observed that the ^{17}O coordination shift for the bound water in $[Rh(H_2O)_6]^{3+}$ was –130.5 ppm.

Table 2. ADF analysis of the diamagnetic (σ_d) and paramagnetic (σ_p) contributions to the total ^{17}O magnetic shielding in two Pt-carboxylate complexes.

	Oxaliplatin		Carboplatin	
	Pt-bound oxygen[a]	Non-coordinated oxygen[a]	Pt-bound oxygen[a]	Non-coordinated oxygen[a]
σ_d(total) (ppm)	394	400	395	402
σ_p(total) (ppm)	–306	–531	–276	–523
σ_p(gauge)	0	–1	1	3
σ_p(occ-occ)	105	20	79	2
σ_p(occ-vir)	–411	–550	–356	–518
	(–156)[b]	(–126)[b]	(–54)[d]	(–66)[d]
	(–48)[c]	(–204)[c]	(4.5)[e]	(–196)[e]

[a]Averaged over the two related oxygen atoms within the same molecule.
[b]From MO#84 and #85 to all virtual MOs.
[c]From MO#92 and #93 to all virtual MOs.
[d]From MO#71 and #75 to all virtual MOs.
[e]From MO#85 and #86 to all virtual MOs.

The origin of ^{17}O coordination shifts

To better understand the very large ^{17}O coordination shift, we decided to carefully examine the ^{17}O NMR tensors. To aid discussion, we label the tensor components according to their directions with respect to the carboxylate plane. As shown in Fig. 5, the in-plane tensor components parallel and perpendicular to the C–O bond are denoted as ∥ and ⊥, respectively, while the tensor component perpendicular to the O–C–O–Pt plane is defined as π. Figure 5 illustrates the changes in tensor components between the two types of oxygen atoms. This analysis immediately reveals that while all three components of the ^{17}O QC tensors change considerably upon Pt coordination, the change in the ∥ component of the ^{17}O CS tensor is significantly larger than those in the other two components. Furthermore, because of the large change

Fig. 6. A partial energy level diagram and selected occupied (84, 85, 92 and 93) and unoccupied (97 and 114) MOs obtained for oxaliplatin from ADF calculations. The ‖ direction for each of the C-O moieties is marked with an arrow in the occupied MOs.

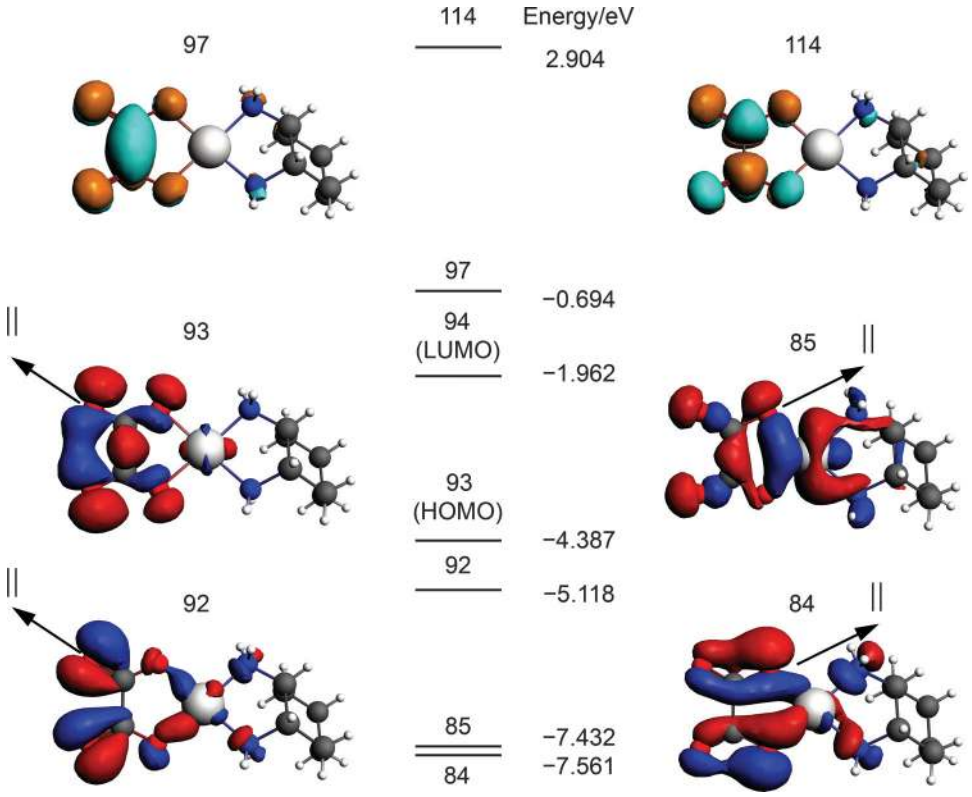

in the ‖ component, the orientations of the δ_{11} and δ_{22} components in the molecular frame of reference appear switched between the directly bonded and non-Pt-coordinated oxygen atoms. As a result, a "cross-over" effect is seen in Fig. 5. A similar "δ_{11}-δ_{22} cross-over" effect was previously reported for the phenolic oxygen atom of tyrosine between the protonated and deprotonated states.[64]

To further identify the origin of the observed ^{17}O coordination shift in terms of specific molecular orbitals (MOs), we performed a detailed magnetic shielding analysis using the ADF program.[46] According to the Ramsey formalism of nuclear magnetic shielding,[65] the total magnetic shielding at a nucleus can be divided into diamagnetic and paramagnetic contributions:

$$(1) \qquad \sigma_{total} = \sigma_d + \sigma_p$$

In general, the diamagnetic shielding term is dominated by core electrons and consequently exhibits essentially no orientation dependence. In contrast, the paramagnetic shielding contribution is responsible for the anisotropic nature of the magnetic shielding tensor. In the formulation implemented in the ADF software package, σ_p is further partitioned into three different parts:[46]

$$(2) \qquad \sigma_p = \sigma_p(\text{gauge}) + \sigma_p(\text{occ-occ}) + \sigma_p(\text{occ-vir})$$

where σ_p(gauge), σ_p(occ-occ), and σ_p(occ-vir) denote the paramagnetic shielding contributions from the gauge, magnetic coupling among occupied MOs, and magnetic coupling between occupied and virtual MOs, respectively. Table 2 lists a summary of individual shielding contributions in oxaliplatin and carboplatin. It is quite clear that σ_p is indeed responsible for the observed coordination shift in Pt-carboxylate complexes. Furthermore, σ_p(occ-vir) makes the largest contribution to σ_p. So what kind of occupied and unoccupied MOs can be magnetically coupled to induce a large paramagnetic shielding effect when the magnetic field is along the C-O bond (that is, the ‖ direction)? It is also well-known from Ramsey's theory[65] that the paramagnetic shielding contribution from magnetic coupling of a pair of occupied and virtual MOs is inversely proportional to the energy gap between them, provided that the two MOs satisfy the symmetry requirement.[66] Previous ^{17}O NMR studies of C–O and N–O compounds have shown[56,57,64,67] that the high-lying nonbonding orbitals (electron lone pairs) on the oxygen atom often make the largest paramagnetic shielding contribution. Use oxaliplatin as an example. As seen in Fig. 6, MO#92 and #93(HOMO) are largely localized on the non-Pt-coordinated oxygen atoms, each having a similar shape as a pure 2p atomic orbital perpendicular to the C–O bond. The ADF analysis showed that the magnetic coupling between these two MOs and all virtual MOs contributes –204 and –48 ppm of paramagnetic shielding for the non-Pt-coordinated and directly Pt-bonded oxygen atoms, respectively (see Table 2). We also found that the magnetic coupling between MO#84 and #85 and all virtual MOs makes comparable paramagnetic shielding contributions on both types of oxygen atoms. Among the virtual MOs, the most important ones are of the π^* type such as MO#97 and #114, which can be magnetically coupled with MO#84, #85, #92, and #93 when the magnetic field lies along the ‖ direction, as also shown in Fig. 6. So the above discussion has shown quite clearly that the large ^{17}O coordination shift observed in the Pt-carboxylate complexes is due to the significantly reduced paramagnetic shielding contribution on the directly Pt-bonded oxygen atom when the magnetic field is along the ‖ direction, which couples MO#92 and #93 with all virtual MOs with the right symmetry.

Conclusions

We have synthesized two ^{17}O-labled platinum-carboxylate complexes (carboplatin and oxaliplatin) that are well-known antican-

cer drugs and carried out solid-state ^{17}O NMR experiments to determine the complete ^{17}O CS and QC tensors in these compounds. We found that the ^{17}O CS and QC tensors for the 2 oxygen atoms within the same carboxylate group are very different, reflecting the monodentate mode of binding between the carboxylate group and Pt(II), i.e., O=C–O–Pt. The observed large coordination shifts of 200 ppm in carboplatin and oxaliplatin are the largest reported to date in ^{17}O NMR studies. By examining the tensor orientations in the molecular frame of reference, we have determined the origin of such large ^{17}O coordination shifts in these Pt-carboxylate complexes. This is a good example to illustrate that ^{17}O CS and QC tensors often provide complementary information about the chemical bonding. It is certainly an advantage of solid-state ^{17}O NMR spectroscopy that these tensor properties can be measured simultaneously. The experimental solid-state ^{17}O NMR results were very well reproduced by plane wave DFT calculations. The demonstrated sensitivity of ^{17}O NMR tensors toward metal-ligand interactions makes ^{17}O NMR a useful tool for studying other metallodrugs. It may also be possible to use solid-state ^{17}O NMR to probe polymorphism of drug compounds.

Supporting information

Supplementary data are available with the article through the journal Web site at http://nrcresearchpress.com/doi/suppl/10.1139/cjc-2015-0019.

Acknowledgements

This work was supported by the Natural Sciences and Engineering Research Council (NSERC) of Canada. Access to the 900 MHz NMR spectrometer and CASTEP software was provided by the National Ultrahigh Field NMR Facility for Solids (Ottawa, Canada), a national research facility supported by a consortium of Canadian universities, National Research Council Canada and Bruker BioSpin and managed by the University of Ottawa (http://nmr900.ca).

References

(1) Lemaitre, V.; Smith, M. E.; Watts, A. *Solid State Nucl. Magn. Reson.* **2004**, *26*, 215. doi:10.1016/j.ssnmr.2004.04.004.
(2) Wu, G. *Prog. Nucl. Magn. Reson. Spectrosc.* **2008**, *52*, 118. doi:10.1016/j.pnmrs.2007.07.004.
(3) Wu, G. *Oxygen-17 NMR Studies of Organic and Biological Molecules*; In *NMR of Quadrupolar Nuclei in Solid Materials*; Wasylishen, R. E.; Ashbrook, S. E.; Wimperis, S., Eds.; John Wiley & Sons Ltd.: Chichester, U.K., 2012; pp. 273–290.
(4) Wong, A.; Poli, F. *Annu. Rep. NMR Spectrosc.* **2014**, *83*, 145. doi:10.1016/B978-0-12-800183-7.00003-4.
(5) Zhu, J.; Ye, E.; Terskikh, V.; Wu, G. *Angew. Chem., Int. Ed.* **2010**, *49*, 8399. doi:10.1002/anie.201002041.
(6) Kong, X.; O'Dell, L. A.; Terskikh, V.; Ye, E.; Wang, R.; Wu, G. *J. Am. Chem. Soc.* **2012**, *134*, 14609. doi:10.1021/ja306227p.
(7) Kong, X.; Shan, M.; Terskikh, V.; Hung, I.; Gan, Z.; Wu, G. *J. Phys. Chem. B* **2013**, *117*, 9643. doi:10.1021/jp405233f.
(8) Vogt, F. G.; Yin, H.; Forcino, R. G.; Wu, L. *Mol. Pharmaceutics* **2013**, *10*, 3433. doi:10.1021/mp400275w.
(9) Kong, X.; Terskikh, V.; Khade, R. L.; Yang, L.; Rorick, A.; Zhang, Y.; He, P.; Huang, Y.; Wu, G. *Angew Chem., Int. Ed.* **2015**. In press. doi:10.1002/anie.201409888.
(10) Michaelis, V. K.; Markhasin, E.; Daviso, E.; Herzfeld, J.; Griffin, R. G. *J. Phys. Chem. Lett.* **2012**, *3*, 2030. doi:10.1021/jz300742w.
(11) Michaelis, V. K.; Corzilius, B.; Smith, A. A.; Griffin, R. G. *J. Phys. Chem. B* **2013**, *117*, 14894. doi:10.1021/jp408440z.
(12) Blanc, F.; Sperrin, L.; Jefferson, D. A.; Pawsey, S.; Rosay, M.; Grey, C. P. *J. Am. Chem. Soc.* **2013**, *135*, 2975. doi:10.1021/ja4004377.
(13) Wheate, N. J.; Walker, S.; Craig, G. E.; Oun, R. *Dalton Trans.* **2010**, *39*, 8113. doi:10.1039/c0dt00292e.
(14) Berners-Price, S. J.; Ronconi, L.; Sadler, P. J. *Prog. Nucl. Magn. Reson. Spectrosc.* **2006**, *49*, 65. doi:10.1016/j.pnmrs.2006.05.002.
(15) Vinje, J.; Sletten, E. *Anticancer Agents Med. Chem.* **2007**, *7*, 35. doi:10.2174/187152007779313982.
(16) Reeder, F.; Guo, Z.; Murdoch, P. D. S.; Corazza, A.; Hambley, T. W.; Berners-Price, S. J.; Chottard, J.-C.; Sadler, P. J. *Eur. J. Biochem.* **1997**, *249*, 370. doi:10.1111/j.1432-1033.1997.00370.x.
(17) Guo, Z.; Habtemariam, A.; Sadler, P. J.; Palmer, R.; Potter, B. S. *New J. Chem.* **1998**, *22*, 11. doi:10.1039/a706739i.
(18) Jensen, M.; Bjerring, M.; Nielsen, N. C.; Nerdal, W. *J. Biol. Inorg. Chem.* **2010**, *15*, 213. doi:10.1007/s00775-009-0586-5.
(19) Lucier, B. E. G.; Reidel, A. R.; Schurko, R. W. *Can. J. Chem.* **2011**, *89*, 919. doi:10.1139/v11-033.
(20) Dong, S.; Yamada, K.; Wu, G. Z. *Naturforsch. A* **2000**, *55*, 21. doi:10.1515/zna-2000-1-205.
(21) Wu, G.; Dong, S. *J. Am. Chem. Soc.* **2001**, *123*, 9119. doi:10.1021/ja0102181.
(22) Wu, G.; Yamada, K. *Solid State Nucl. Magn. Reson.* **2003**, *24*, 196. doi:10.1016/S0926-2040(03)00046-8.
(23) Zhang, Q. W.; Chekmenev, E. Y.; Wittebort, R. J. *J. Am. Chem. Soc.* **2003**, *125*, 9140. doi:10.1021/ja034495e.
(24) Lemaitre, V.; Pike, K. J.; Watts, A.; Anupold, T.; Samoson, A.; Smith, M. E.; Dupree, R. *Chem. Phys. Lett.* **2003**, *371*, 91. doi:10.1016/S0009-2614(03)00254-9.
(25) Pike, K. J.; Lemaitre, V.; Kukol, A.; Anupold, T.; Samoson, A.; Howes, A. P.; Watts, A.; Smith, M. E.; Dupree, R. *J. Phys. Chem. B* **2004**, *108*, 9256. doi:10.1021/jp049958x.
(26) Yates, J. R.; Pickard, C. J.; Payne, M. C.; Dupree, R.; Profeta, M.; Mauri, F. *J. Phys. Chem. A* **2004**, *108*, 6032. doi:10.1021/jp049362+.
(27) Gervais, C.; Dupree, R.; Pike, K. J.; Bonhomme, C.; Profeta, M.; Pickard, C. J.; Mauri, F. *J. Phys. Chem. A* **2005**, *109*, 6960. doi:10.1021/jp0513925.
(28) Wong, A.; Pike, K. J.; Jenkins, R.; Clarkson, G. J.; Anupold, T.; Howes, A. P.; Crout, D. H. G.; Samoson, A.; Dupree, R.; Smith, M. E. *J. Phys. Chem. A* **2006**, *110*, 1824. doi:10.1021/jp055807y.
(29) Howes, A. P.; Anupold, T.; Lemaitre, V.; Kukol, A.; Watts, A.; Samoson, A.; Smith, M. E.; Dupree, R. *Chem. Phys. Lett.* **2006**, *421*, 42. doi:10.1016/j.cplett.2006.01.061.
(30) Wong, A.; Howes, A. P.; Pike, K. J.; Lemaitre, V.; Watts, A.; Anupold, T.; Past, J.; Samoson, A.; Dupree, R.; Smith, M. E. *J. Am. Chem. Soc.* **2006**, *128*, 7744. doi:10.1021/ja062031l.
(31) Wong, A.; Thurgood, G.; Dupree, R.; Smith, M. E. *Chem. Phys.* **2007**, *337*, 144. doi:10.1016/j.chemphys.2007.07.007.
(32) Wong, A.; Howes, A. P.; Yates, J. R.; Watts, A.; Anupold, T.; Past, J.; Samoson, A.; Dupree, R.; Smith, M. E. *Phys. Chem. Chem. Phys.* **2011**, *13*, 12213. doi:10.1039/c1cp20629j.
(33) Hagaman, E. W.; Chen, B.; Jiao, J.; Parsons, W. *Solid State Nucl. Magn. Reson.* **2012**, *41*, 60. doi:10.1016/j.ssnmr.2011.12.001.
(34) Rees, G. J.; Day, S. P.; Lari, A.; Howes, A. P.; Iuga, D.; Pitak, M. B.; Coles, S. J.; Threlfall, T. L.; Light, M. E.; Smith, M. E.; Quigley, D.; Wallis, J. D.; Hanna, J. V. *CrystEngComm* **2013**, *15*, 8823. doi:10.1039/c3ce41258j.
(35) He, P.; Xu, J.; Terskikh, V. V.; Sutrisno, A.; Nie, H. Y.; Huang, Y. *J. Phys. Chem. C* **2013**, *117*, 16953. doi:10.1021/jp403512m.
(36) Beagley, B.; Cruickshank, D. W. J.; McAuliffe, C. A.; Pritchard, R. G.; Beddoes, R. L.; Cernik, R. J.; Mills, O. S. *J. Mol. Struct.* **1985**, *130*, 97. doi:10.1016/0022-2860(85)85025-0.
(37) Bruck, M. A.; Bau, R.; Noji, M.; Inagaki, K.; Kindani, Y. *Inorg. Chim. Acta* **1984**, *92*, 279. doi:10.1016/S0020-1693(00)80051-1.
(38) Rochon, F. D.; Massarweh, G. *Inorg. Chim. Acta* **2006**, *359*, 4095. doi:10.1016/j.ica.2006.04.014.
(39) Habala, L.; Galanski, M.; Yasemi, A.; Nazarov, A. A.; Graf v. Keyserlingk, N. G.; Keppler, B. K. *Eur. J. Med. Chem.* **2005**, *40*, 1149. doi:10.1016/j.ejmech.2005.06.003.
(40) Massiot, D.; Fayon, F.; Capron, M.; King, I.; Le Calve, S.; Alonso, B.; Durand, J.-O.; Bujoli, B.; Gan, Z.; Hoatson, G. *Magn. Reson. Chem.* **2002**, *40*, 70. doi:10.1002/mrc.984.
(41) Clark, S. J.; Segall, M. D.; Pickard, C. J.; Hasnip, P. J.; Refson, K.; Probert, M. J.; Payne, M. C. *Z. Kristallogr.* **2005**, *220*, 567. doi:10.1524/zkri.220.5.567.65075.
(42) Profeta, M.; Mauri, F.; Pickard, C. J. *J. Am. Chem. Soc.* **2003**, *125*, 541. doi:10.1021/ja027124r.
(43) Perdew, J. P.; Burke, K.; Ernzerhof, M. *Phys. Rev. Lett.* **1996**, *77*, 3865. doi:10.1103/PhysRevLett.77.3865.
(44) Perdew, J. P.; Burke, K.; Ernzerhof, M. *Phys. Rev. Lett.* **1998**, *80*, 891. doi:10.1103/PhysRevLett.80.891.
(45) Pfrommer, B. G.; Cote, M. G. L. S.; Cohen, M. L. *J. Comput. Phys.* **1997**, *131*, 233. doi:10.1006/jcph.1996.5612.
(46) Te Velde, G.; Bickelhaupt, F. M.; Baerends, E. J.; Fonseca Guerra, C.; Van Gisbergen, S. J. A.; Snijders, J. G.; Ziegler, T. *J. Comput. Chem.* **2001**, *22*, 931. doi:10.1002/jcc.1056.
(47) Vosko, S. H.; Wilk, L.; Nusair, M. *Can. J. Phys.* **1980**, *58*, 1200. doi:10.1139/p80-159.
(48) van Lenthe, E.; Baerends, E. J.; Snijders, J. G. *J. Chem. Phys.* **1993**, *99*, 4597. doi:10.1063/1.466059.
(49) van Lenthe, E.; Baerends, E. J.; Snijders, J. G. *J. Chem. Phys.* **1994**, *101*, 9783. doi:10.1063/1.467943.
(50) van Lenthe, E.; Snijders, J. G.; Baerends, E. J. *J. Chem. Phys.* **1996**, *105*, 6505. doi:10.1063/1.472460.
(51) Van Lenthe, E.; Van Leeuwen, R.; Baerends, E. J.; Snijders, J. G. *Int. J. Quantum Chem.* **1996**, *57*, 281. doi:10.1002/(SICI)1097-461X(1996)57:3<281::AID-QUA2>3.0.CO;2-U.
(52) Yamada, K.; Dong, S.; Wu, G. *J. Am. Chem. Soc.* **2000**, *122*, 11602. doi:10.1021/ja0008315.
(53) Bryce, D. L.; Wasylishen, R. E. In *NMR of Quadrupolar Nuclei in Solid Materials*; Wasylishen, R. E.; Ashbrook, S. E.; Wimperis, S., Eds.; John Wiley & Sons Ltd., Chichester, UK, 2012; Chapter 4.
(54) Kwan, I. C. M.; Mo, X.; Wu, G. *J. Am. Chem. Soc.* **2007**, *129*, 2398. doi:10.1021/ja067991m.
(55) Wu, G.; Dong, S.; Ida, R.; Reen, N. *J. Am. Chem. Soc.* **2002**, *124*, 1768. doi:10.1021/ja011625f.

(56) Zhu, J.; Geris, A. J.; Wu, G. *Phys. Chem. Chem. Phys.* **2009**, *11*, 6972. doi:10.1039/b906438a.
(57) Wu, G.; Zhu, J. F.; Mo, X.; Wang, R. Y.; Terskikh, V. *J. Am. Chem. Soc.* **2010**, *132*, 5143. doi:10.1021/ja909656w.
(58) Zhu, J.; Wu, G. *J. Am. Chem. Soc.* **2011**, *133*, 920. doi:10.1021/ja1079207.
(59) Jackson, J. A.; Lemons, J. F.; Taube, H. *J. Chem. Phys.* **1960**, *32*, 553. doi:10.1063/1.1730733.
(60) Glass, G. E.; Schwabacher, W. B.; Tobias, R. S. *Inorg. Chem.* **1968**, *7*, 2471. doi:10.1021/ic50070a001.
(61) Fedotov, M. A.; Troitskii, S. Y.; Likholobov, V. A. *Koord. Khim.* **1990**, *16*, 1675.
(62) Laurenczy, G.; Rapaport, I.; Zbinden, D.; Merbach, A. E. *Magn. Reson. Chem.* **1991**, *29*, S45. doi:10.1002/mrc.1260291311.
(63) Drljaca, A.; Zahl, A.; van Eldik, R. *Inorg. Chem.* **1998**, *37*, 3948. doi:10.1021/ic971074n.
(64) Zhu, J.; Lau, J. Y. C.; Wu, G. *J. Phys. Chem. B* **2010**, *114*, 11681. doi:10.1021/jp1055123.
(65) Ramsey, N. F. *Phys. Rev.* **1950**, *78*, 699. doi:10.1103/PhysRev.78.699.
(66) Jameson, C. J.; Gutowsky, H. S. *J. Chem. Phys.* **1964**, *40*, 1714. doi:10.1063/1.1725387.
(67) Wu, G.; Mason, P.; Mo, X.; Terskikh, V. *J. Phys. Chem. A* **2008**, *112*, 1024. doi:10.1021/jp077558e.